https://doi.org/10.48047/AFJBS.6.15.2024.192-212

African Journal of Biological Sciences

Journal homepage: http://www.afjbs.com

Research Paper Open Access

Isolation and identification of potent antidiabetic compounds from *Syzygium zeylanicum* . (L.)DC. using *in silico* docking and Molecular Dynamics Approaches

Anjali Nair G[1], P. Maheshwari*[2]

[1]Research scholar, School of Pharmaceutical Sciences, Department of Pharmacy Practice, School of Pharmaceutical Sciences, Vels Institute of Science, Technology and Advanced Studies (VISTAS) Pallavaram, Chennai, India

[2]Associate Professor, Department of Pharmacy Practice, School of Pharmaceutical Sciences, Vels Institute of Science, Technology and Advanced Studies (VISTAS)

Pallavaram, Chennai, India

Corresponding author: Dr.P Maheshwari, Associate Professor

Department of Pharmacy Practice, School of Pharmaceutical Sciences, Vels Institute of Science, Technology and Advanced Studies (VISTAS)

Pallavaram, Chennai, India E-mail: mahe.mpharm@gmail.comTel.: +91 96771 92659

Volume 6, Issue 15, Aug 2024

Received: 15 June 2024

Accepted: 25 July 2024

Published: 15 Aug 2024

doi: 10.48047/AFJBS.6.15.2024.192-212

ABSTRACT

Syzygium zeylanicum (L.) DC (S. zeylanicum) is a member of the Myrtaceae family. Phytochemicals found in the plant, such as flavonoids, phenols, and saponin, may have antioxidant and anti-diabetic properties. A flavonoid, 2,3,13,14,15-penta hydroxyl 5,11-dioxo1,2,3,4,4a,5,6,7,10,11,16,16 and dodeca hydro-6,10-epoxy dibenzo[a,d][12]annulen7-yl 3oxo-4-(2,3,4-trihydroxycyclhexyl)butanoate, were isolated from *Syzygium zeylanicum* by column chromatography and characterized using advanced analytical techniques such as ^{1}H NMR, ^{13}C NMR, mass spectrometry, and FT-IR. This flavonoid was screened *in-silico* against antidiabetic targets viz., α-Amylase, α-Glucosidase, Peroxisome proliferator-activated receptor gamma (PPAR-γ), Glycogen synthase kinase 3-beta (GSK3-β), Dipeptidyl peptidase-4 (DPP-4), Fibroblast growth factor (FGF), and Matrix metalloproteinase-1 (MMP-1). Molecular dynamics simulation and binding affinity analysis suggested that the ligand exhibits strong and stable binding with several critical proteins involved in glucose metabolism and insulin regulation. The potential of this ligand to inhibit these enzymes makes it a promising candidate for developing novel therapeutic agents for diabetes and related metabolic disorders. The overall binding profile supports the potential of the compound as an antidiabetic agent via multiple mechanisms, including enzyme inhibition, enhanced insulin secretion, and improved insulin sensitivity. Further experimental validation is necessary to confirm these predictions and elucidate the pharmacological effects of the compound.

KEYWORDS: column chromatography, *in-silico,* Molecular dynamics simulation, antidiabetic

INTRODUCTION

Diabetes mellitus (DM) is a chronic metabolic disorder characterized by persistent hyperglycaemia resulting from defects in insulin secretion, insulin action, or both. This condition is a major public health concern worldwide, affecting millions of people (American Diabetes Association, 2009). The World Health Organization (WHO) reported that over 422 million adults were affected by diabetes in 2020, with the number expected to increase significantly in the coming decades (Khawandanah, 2019). Diabetes is primarily classified into type 1, an autoimmune condition, and type 2, which is more common and results from insulin resistance along with gestational and other specific forms (Galicia-Garcia *et al*., 2020).

The global diabetes burden is rapidly increasing, with 4.2 million deaths and over $760 billion in healthcare costs in 2019, driven by rising rates of type 2 diabetes due to lifestyle changes, obesity, and aging population. This trend highlights the urgent need for more effective prevention and treatment strategies, particularly in low-income and middle-income countries (Khan *et al*., 2020; Saeedi *et al*., 2019).

Current diabetes treatments focus on maintaining normal blood glucose levels, with insulin therapy as the mainstay for type 1 diabetes and a combination of lifestyle modifications and pharmacotherapy, such as metformin and SGLT-2 inhibitors, for type 2 diabetes (Aloke *et al*., 2022). Despite advancements, these therapies primarily manage symptoms rather than addressing the root causes, such as insulin resistance and beta-cell dysfunction, and are often associated with side effects, such as hypoglycaemia, weight gain, and cardiovascular risks (Weinberg Sibony *et al*., 2023). As a result, interest in herbal medicines has grown, with plants offering diverse bioactive compounds, including flavonoids and alkaloids, which show promising hypoglycemic effects and are perceived as safer alternatives for long-term management (Evans *et al*., 2020).

Several plants have demonstrated promising antidiabetic properties via various mechanisms. *Momordica charantia* (bitter melon) enhances glucose uptake and insulin sensitivity, while *Trigonella foenum-graecum* (fenugreek) improves glycaemic control by slowing carbohydrate absorption and boosting insulin action. *Gymnema sylvestre*, known as the "sugar destroyer," suppresses sweetness and modulates glucose metabolism (Alam *et al*. 2022). Other plants, such as *Pterocarpus marsupium, Aloe vera, Berberis aristata,* and *Salacia oblonga*, have shown antidiabetic activity by regenerating beta cells, inhibiting glucose absorption, or modulating insulin

signalling, highlighting their potential as adjuncts or alternatives to conventional treatments (Ota & Ulrih, 2017).

Among these herbal approaches, *Syzygium zeylanicum* (commonly known as the Indian clove) has attracted attention because of its traditional use in treating various ailments, including diabetes (Nair & Maheshwari, 2024). Syzygium species are widely known for their medicinal properties, with *Syzygium cumini* (jamun) being particularly well known for its antidiabetic effects (Nguyen *et al*., 2024). Various studies have identified phytochemicals in Syzygium species, such as polyphenols, flavonoids, and tannins, which exhibit antioxidant, anti-inflammatory, and insulin-sensitizing properties, making them valuable candidates for diabetes management (Shilpa & Krishnakumar, 2023; Govindarajan & Benelli, 2016 and Nomi *et al*., 2012).

This study aimed to explore the anti-diabetic potential of *Syzygium zeylanicum* in response to the need for novel, effective, and safe diabetes therapies. *Syzygium zeylanicum* is relatively underexplored, despite evidence suggesting that it may possess bioactive compounds with significant hypoglycaemic activity. The bioactive compound SZ-I, a flavonoid, was isolated using column chromatography and characterized using IR, NMR, and mass spectrometry. *In silico* molecular docking studies were performed to assess the binding affinity of SZ-I with key diabetes-related proteins, such as α-amylase, α-glucosidase, GLP-1, PPAR-γ, GSK3-β, DPP-4, FGF, and MMP-1, providing insights into its possible mechanisms of action and laying the groundwork for further in vivo and clinical research.

MATERIALS AND METHODS

Plant material

Plant samples were collected in October from the Mahatma Gandhi University Campus in the Kottayam district, Kerala, India. Dr. Sreekumar V. B., a senior scientist at the Forest Botany Department of the Kerala Forest Research Institute (KFRI) in Peechi, Thrissur, Kerala, authenticated the samples. The specimen was stored in the KFRI Herbarium (accession number: 18370).

Extraction

Successive solvent extraction was performed for the dried plant material using petroleum ether, chloroform, ethyl acetate, ethanol, and water. Powdered leaf samples (450 g) were first defatted

with petroleum ether in an orbital shaker for 48 h. The extract was filtered through a Whatman No. 1 filter paper and concentrated using a rotary evaporator. This process was repeated using chloroform, ethyl acetate, ethanol, and water (Dokuparthi & Reddy, 2021).

Isolation of Phytoconstituents

A column was prepared with 200 g of silica gel (60/120 mesh size) and carefully packed without air bubbles, using petroleum ether as the packing solvent. The column was left undisturbed for one hour to ensure tight packing. The sample mixture was applied to the top of the stationary phase. The compounds were separated by sequential elution with solvents of increasing polarity, including petroleum ether, chloroform, ethyl acetate, methanol, and water. Each column fraction was collected separately and was concentrated under reduced pressure. Finally, the column was washed with water to ensure the complete elution of the remaining compounds (Singamaneni *et al*., 2020).

Characterization of the isolated compound

The isolated compound was characterized using FT-IR, ^{1}H NMR, ^{13}C NMR, mass spectrometry, and GC-MS techniques to elucidate its chemical structure. FT-IR spectra were recorded using a Shimadzu spectrometer to identify the functional groups and molecular vibrations. Proton (^{1}H) and carbon (^{13}C) NMR spectra were obtained with a Bruker 400 MHz spectrometer, optimizing parameters like pulse angles and repetition times for accurate chemical shift determination, with TMS as reference signal. Mass spectra were recorded using a Shimadzu GC-MS system with electron impact ionization, which provided molecular weight and fragmentation data with high accuracy for compound identification (Dokuparthi *et al*., 2014).

Molecular Docking studies

The molecular docking study of the isolated flavonoid 2,3,13,14,15-penta hydroxyl 5,11-dioxo1,2,3,4,4a,5,6,7,10,11,16,16 and dodeca hydro-6,10-epoxy dibenzo[a,d][12]annulen7-yl 3oxo-4-(2,3,4-trihydroxycyclhexyl)butanoate was conducted using the cDOCKER algorithm of Discovery Studio v3.5 software. The protein structures of the selected diabetes-related targets (Table 1) were retrieved from the Protein Data Bank and prepared by removing water molecules, heteroatoms, and any co-crystallized ligands, followed by the addition of hydrogen atoms and energy minimization using the CHARMM force field. The 3D structure of the flavonoid was

prepared using the same software and energy minimization was applied to obtain a stable conformation. Receptor grids were generated around the active sites of the target proteins to define the search space for ligand docking. The cDOCKER algorithm was then used to flexibly dock the flavonoid into the protein binding pockets, allowing for the exploration of multiple ligand conformations (Sanagala *et al*., 2024 and Thabet *et al*., 2024)

Table 1. Targets selected for Molecular Docking study

Target Enzyme	Abbreviation	PDB ID
α-Amylase	Alpha-Amylase	10SE
α -Glucosidase	Alpha-Glucosidase	5NN3
GLP-1	Glucagon-Like Peptide-1 Receptor	3IOL
PPAR-γ	Peroxisome Proliferator-Activated Receptor Gamma	2F4B
GSK3-β	Glycogen Synthase Kinase-3 Beta	5K5N
DPP-4	Dipeptidyl Peptidase-4	5Y7H
FGF	Fibroblast Growth Factor	5E8W
MMP-1	Matrix Metalloproteinase-1	966C 4XCT

After docking, the best binding positions were selected based on the cDOCKER interaction energy scores. These scores account for various interaction forces, such as van der Waals and electrostatic interactions, as well as internal ligand strains. The docking results were ranked, and the top poses for each target were examined to identify critical interactions, such as hydrogen bonds, hydrophobic interactions, and π-π stacking between the flavonoid and active site residues. The docking study provided insights into the potential of flavonoids to interact with multiple targets related to diabetes, suggesting their ability to modulate key proteins involved in glucose metabolism, insulin sensitivity, and carbohydrate digestion (Fatima & Edupuganti, 2023).

Molecular Dynamics Simulation Study

Simulation Setup: Molecular dynamics simulations were performed using the Desmond software. The protein-ligand complex studied was named the 1ose-Ligand-complex, and the system was prepared with 30,902 atoms, including 7,724 water molecules (Faseela & Maheshwari, 2024). The ligand used in this study had the molecular formula C30H52O14, with 96 atoms in total, 44 of which were heavy. Sodium (Na) and chloride (Cl) ions were added to neutralize the system at

concentrations of 58.848 mM and 49.433 mM, respectively (Macalalad & Gonzales, 2023; Salo-Ahen *et al*., 2021).

Simulation Parameters: The simulation was conducted in an NPT (constant number of particles, pressure, and temperature) ensemble at 300 K for 100.102 ns. To ensure system stability, the pressure was maintained using a barostat, and the temperature was controlled using a thermostat.

Data Analysis

Root Mean Square Deviation (RMSD): RMSD calculations were performed to monitor the stability and conformational changes of both the protein and the ligand throughout the simulation. The protein frames were aligned to the backbone atoms of the reference structure, and the RMSD was calculated for each frame in the trajectory. Ligand RMSD was measured by aligning the protein-ligand complex on the protein backbone and then calculating the RMSD of the ligand heavy atoms.

Root Mean Square Fluctuation (RMSF): The RMSF was calculated to assess the local flexibility of the protein and ligand residues. The protein RMSF provided insights into regions with higher flexibility, whereas the ligand RMSF characterized the fluctuations of individual ligand atoms.

Secondary Structure Analysis: The secondary structure elements (SSE) of the protein were monitored throughout the simulation to observe any changes in alpha-helices, beta-strands, and other structural components. The SSE distribution was analyzed using the residue index and summarized over the trajectory.

Protein–ligand Interactions: Over the course of the simulation, interactions between the protein and ligand were categorized and analyzed. These interactions include hydrogen bonds, hydrophobic contacts, ionic interactions, and water bridges. The frequency and stability of these interactions were visualized using bar charts and timeline representations.

Ligand Torsion Profile: The torsional behavior of the rotatable bonds of the ligand was analyzed to understand the conformational changes and strain experienced by the ligand during simulation. Radial and bar plots were used to summarize torsion angles and their probability densities.

Ligand Properties: Various properties of the ligand, including RMSD, radius of gyration (rGyr), intramolecular hydrogen bonds (intraHB), molecular surface area (MolSA), solvent-accessible

surface area (SASA), and polar surface area (PSA), were calculated to assess the ligand's behavior and interaction with the protein (Fatriansyah *et al*., 2022 and Madej *et al*., 2014).

RESULTS AND DISCUSSIONS

Isolation of Phytochemicals

Column chromatography of the *S. zeylanicum* ethanolic extract yielded various fractions using different solvent systems in a gradient elution process. Initially, fractions F1 to F5 were eluted with 100% petroleum ether, followed by F6 to F10 with a mixture of petroleum ether and chloroform in a 75:25 ratio. Further elution with petroleum ether and chloroform in a 50:50 ratio yielded fractions F11–F15, while fractions F16–F20 were obtained with a 25:75 ratio of the same solvents. Pure chloroform was used to elute F21–F25, followed by a chloroform and ethyl acetate mixture in varying ratios to obtain fractions F26–F40. Pure ethyl acetate was then used to collect F41–F45, with subsequent ethyl acetate and methanol mixtures yielding F46–F60. Methanol alone was used to isolate fractions F61 to F65, followed by methanol and water mixtures for fractions F66 to F80. The compound was successfully isolated from fractions F71–F75 using a 50:50 methanol and water mixture. Finally, pure water was used to elute the remaining fractions F81–F85.

The isolated compound SZ-I, a light-yellow solid weighing 203 mg, exhibited solubility in chloroform, methanol, and ethanol and had a melting point range of 188-195°C. Preliminary tests confirmed that it was a flavonoid. Mass spectrometry analysis determined its mass to be 620 M±1, with the molecular formula $C_{30}H_{36}O_{14}$. TLC using a methanol solvent system (8:2 v/v) revealed an Rf value of 0.45.

This compound was subjected to spectroscopic analysis to elucidate its structure. The IR spectrum shows significant absorption bands at 3451 cm^{-1} for O-H stretching, 3017 cm^{-1} for aromatic C-H stretching, and 1654 cm^{-1} for C=O stretching. The ^{1}H NMR spectrum showed a multiplet at 7 ppm corresponding to aromatic protons, a multiplet at 3.7 ppm for hydroxyl protons, and a multiplet at 1 ppm for CH_2 protons. The ^{13}C NMR spectrum showed peaks at 168 ppm for C=O carbons, 121 ppm for aromatic carbons, and 54 ppm for C-OH carbons. Mass spectrometry revealed a molecular ion peak at m/z = 620. These spectral data confirmed the structure of SZ-I as 2,3,13,14,15-penta hydroxyl 5,11-dioxo-1,2,3,4,4a,5,6,7,10,11,16,16 and dodeca hydro-6,10-epoxy dibenzo[a,d][12]annulen7-yl 3-oxo-4-(2,3,4-trihydroxycyclohexyl)butanoate, respectively.

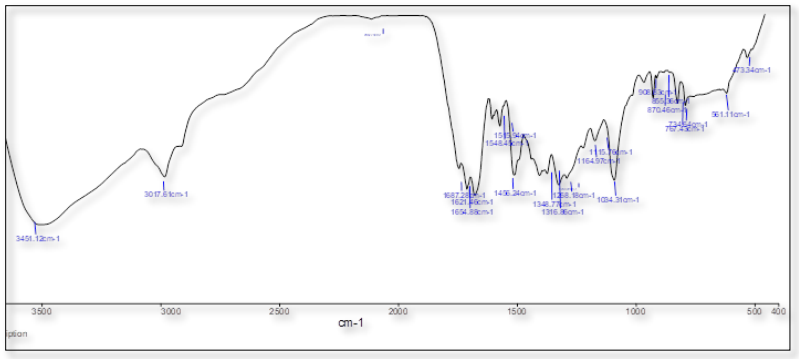

Figure 1. FT-IR Spectrum of SZ-1

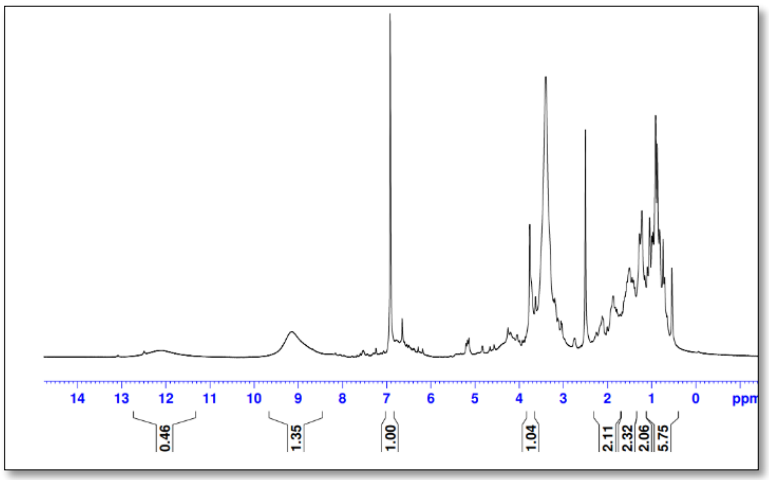

Figure 2. ^{1}H NMR Spectrum of SZ-1

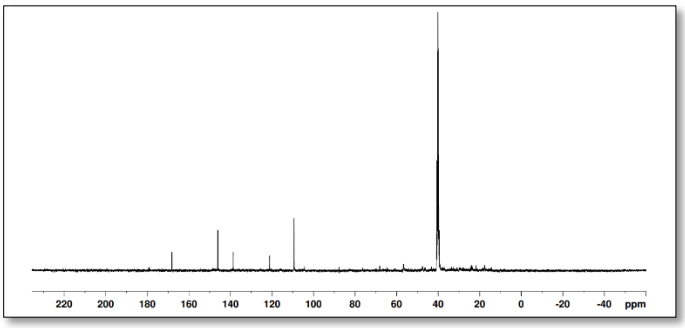

Figure 3. ^{13}C NMR Spectrum of SZ-1

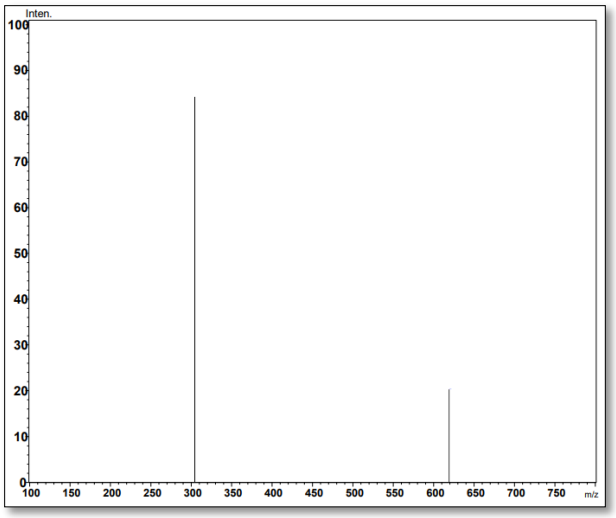

Figure 4. MASS Spectrum of SZ-1

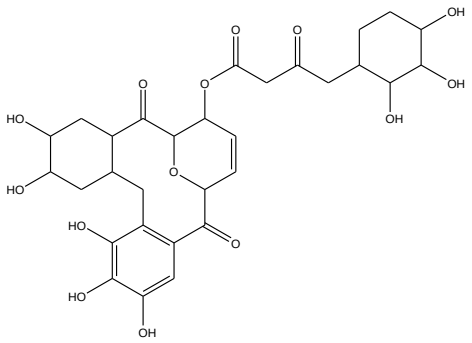

Figure 5. Structure of SZ-1

***In-silico* Molecular Docking Study**

Docking study results indicated that the isolated flavonoid demonstrated significant binding affinities to key diabetes-related proteins through van der Waals interactions and hydrogen bonding. The strongest binding was observed with GSK3-β (PDB ID: 5K5N) with a docking score of -9.8, interacting with residues such as LYS 250, ARG 253, and TYR 248, forming four hydrogen bonds with residues such as SER 245 and PRO 249. This suggests a strong potential for inhibiting GSK3-β, which could enhance glycogen synthesis and improve glucose metabolism. The flavonoid also showed good binding to α-amylase (PDB ID: 10SE) with a docking score of -9.1, forming three hydrogen bonds with residues such as SER 289 and ASP 402, indicating its potential to inhibit carbohydrate digestion and manage postprandial blood glucose levels (Table 2 and Figure 6).

Additionally, the compound exhibited a docking score of -9.3 against FGF (PDB ID: 5E8W), interacting with residues such as VAL 219 and ASP 351, forming five hydrogen bonds with ARG 215 and SER 434, suggesting a role in modulating glucose and lipid metabolism. Binding to PPAR-γ (PDB ID: 2F4B) with a score of -8.8 and forming five hydrogen bonds implies the potential for improving insulin sensitivity. The flavonoid also demonstrated moderate binding to other targets, such as α-glucosidase, GLP-1, DPP-4, and MMP-1, indicating its multi-target action in modulating pathways relevant to diabetes, including glucose absorption, insulin secretion, and tissue remodeling.

The strongest binding to GSK3-β suggests that it may play a primary role in improving insulin sensitivity and enhancing glycogen synthesis, which is critical for maintaining blood glucose levels in patients with diabetes. GSK3-β inhibition has been a focus of diabetes research because it impacts insulin signaling and glucose homeostasis. Additionally, the inhibition of alpha-amylase by flavonoids supports the control of postprandial glucose levels by reducing carbohydrate digestion and further stabilizing blood sugar levels.

Furthermore, the interaction between FGFR and PPAR-γ indicates that flavonoids may have a broader metabolic influence. They improve insulin sensitivity and regulate lipid metabolism, which are beneficial for managing glucose levels and reducing the risk of complications in patients with diabetes. These multi-target effects suggest that flavonoids could serve as comprehensive therapeutic agents for diabetes management by targeting different mechanisms involved in glucose regulation, insulin sensitivity, and metabolism.

Table 2. Molecular Docking study results of the isolated flavonoid

Target Protein	PDB Id	Docking Score	Van Der Waals Interactions	No. of Hydrogen Bonds	Hydrogen Interaction
α-Amylase	10SE	-9.1	GLY 334, ASP 290, ARG 421, GLY 403, ALA 3,GLY 9, SER 8	03	SER 289,ASP 402, ARG 10
α -Glucosidase	5NN3	-7.9	THR 333, GLN 244, GLY 334, LEU 538, GLU 471, GLY 473, HIS 562, SER	04	ARG 190, ASN 470, THR 469

			560, THR 567, SER 566, LEU 565		
GLP-1	3IOL	-7.7	VAL 83, SER 49, ASP 53, PRO 56, PRO 54, PHE 61, GLY 75, ASN 82	06	PHE 80, SER 79, GLU 76,CYS 71, ARG 64
PPAR-γ	2F4B	-8.8	ILE 456, PHE 360,PHE 282, SER 464, LEU 465,MET 463	05	ARG 357,LYS 275, ASP 462, THR 461
GSK3-β	5K5N	-9.8	LYS 250, ARG 253, ILE 236, LEU 235, PRO 234, TYR 248,VAL 262, ALA 261, GLY 260, PRO 674, LEU 680, ARG 684,GLN 247, LEU 246	04	SER 245, PRO 249, THR 251, GLU 237
DPP-4	5Y7H	-7.7	GLY 45, ASP 105, LEU 112, ILE 100	02	LEU 104, GLU 208, LYS 184, HIS 203, GLU 174, HIS 175
FGF	5E8W	-9.3	VAL 219, LYS 213, ASP 351, GLY 214, LYS 335, ASP 333, LYS 376, TYR 378, ASP 435, LEU 426, GLN 425	05	ARG 215, SER 434, ARG 377, VAL 432
MMP-1	4XCT	-7.9	LYS 184, LEU 209, GLU 208, ASP 206 GLU 130, HIS 175, GLU 174, HIS 203, ALA 173, GLY 171	07	ASP 131, ASP 131, ASN 171, PHE 170, GLN 169, VAL 172

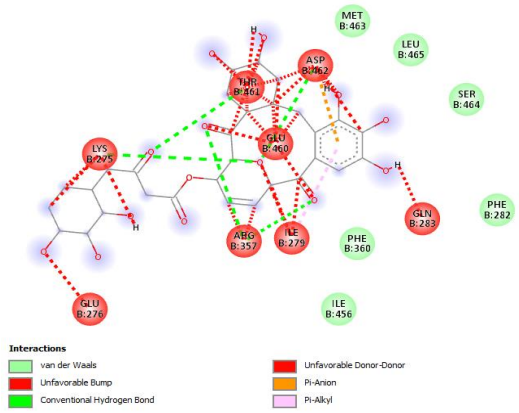

PPAR-γ

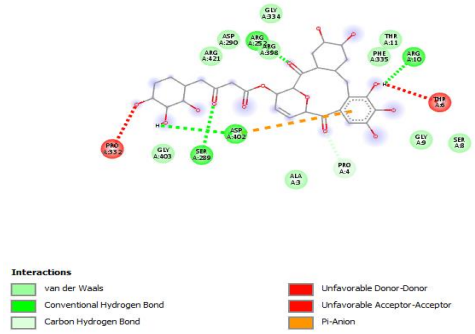

α-Amylase

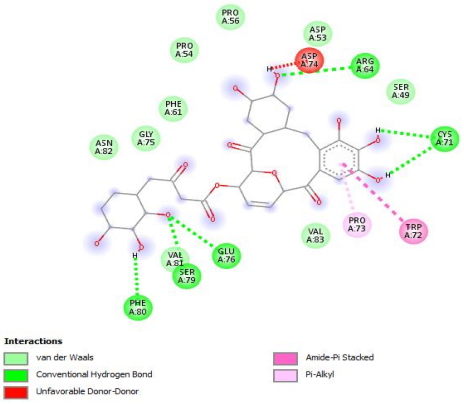

GLP-1

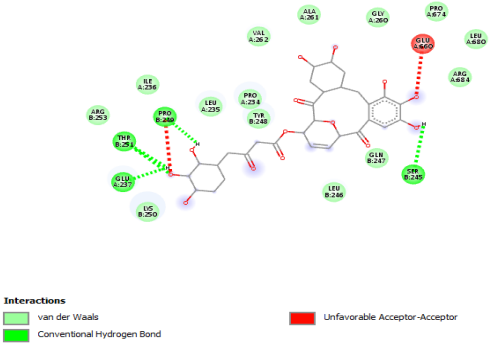

DPP-4

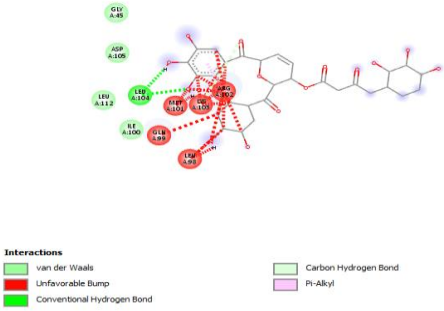

GSK3-β

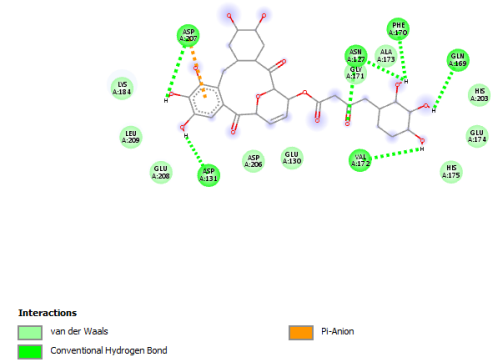

MMP-1

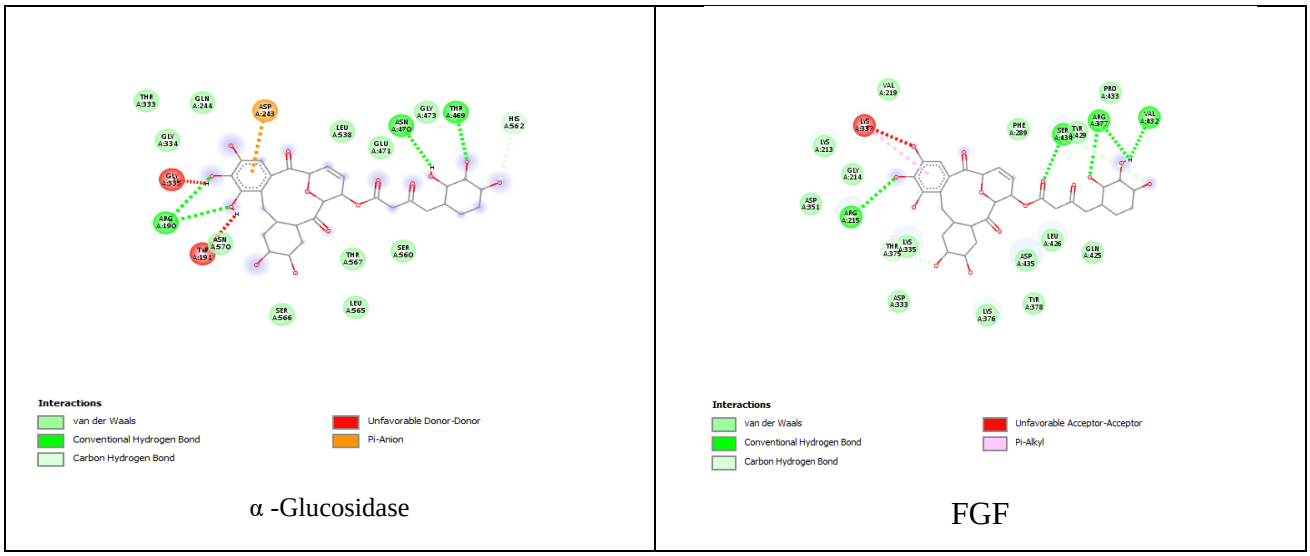

Figure 6. 2D interactions of the flavonoid with the targets

Molecular Dynamics Simulation Study

Stability and Conformational Analysis

Protein RMSD: RMSD analysis indicated that the protein maintained structural stability throughout the 100.102 ns simulation. The RMSD values showed minor fluctuations, stabilizing towards the end, suggesting that the protein reached equilibrium without significant conformational changes (Figure 7).

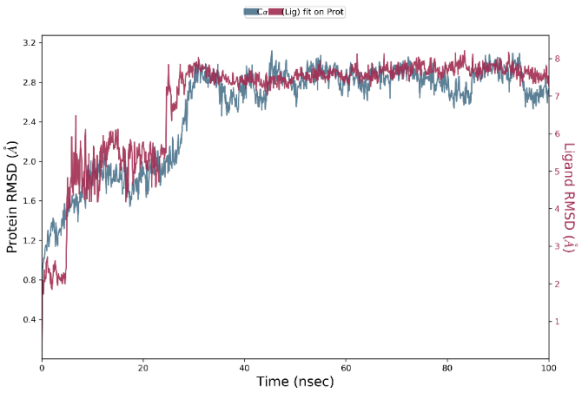

Figure 7. Protein RMSD

Ligand RMSD: The ligand RMSD relative to the protein demonstrated that the ligand remained stable within the binding pocket. Low and stable RMSD values indicate a strong and stable binding interaction between the ligand and protein.

Flexibility and Interaction Dynamics

Protein RMSF: The RMSF plot revealed that the N- and C-terminal regions of the protein exhibited higher flexibility, whereas the secondary structural elements, such as alpha-helices and beta-strands, remained more rigid. This observation is consistent with typical protein dynamics, where loop regions show more fluctuations than structured regions (Figure 8).

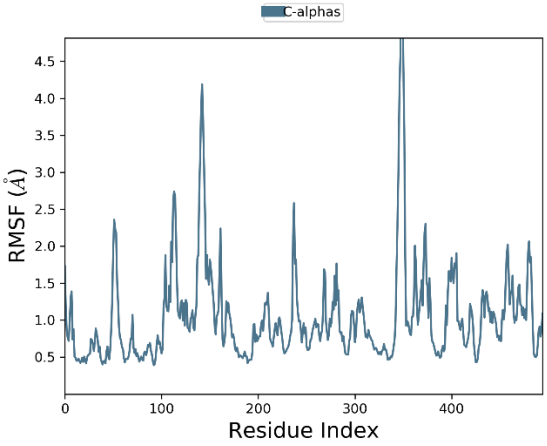

Figure 8. Protein RMSF

Ligand RMSF: The ligand RMSF data indicated that certain ligand atoms exhibited higher fluctuations, reflecting their flexibility and dynamic interactions with the protein-binding site (Figure 9).

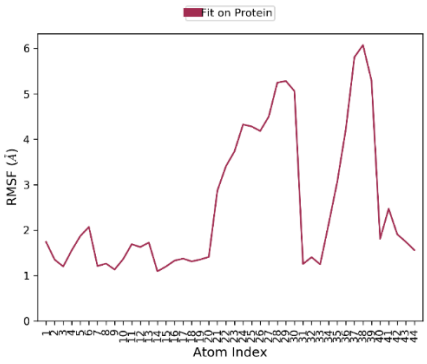

Figure 9. Ligand RMSF

Secondary Structure Stability

Secondary Structure Elements: The Secondary structure analysis showed that the protein maintained its overall secondary structure throughout the simulation. The percentage of alpha

helices (15.24%) and beta strands (18.39%) remained consistent, indicating structural integrity (Figure 10).

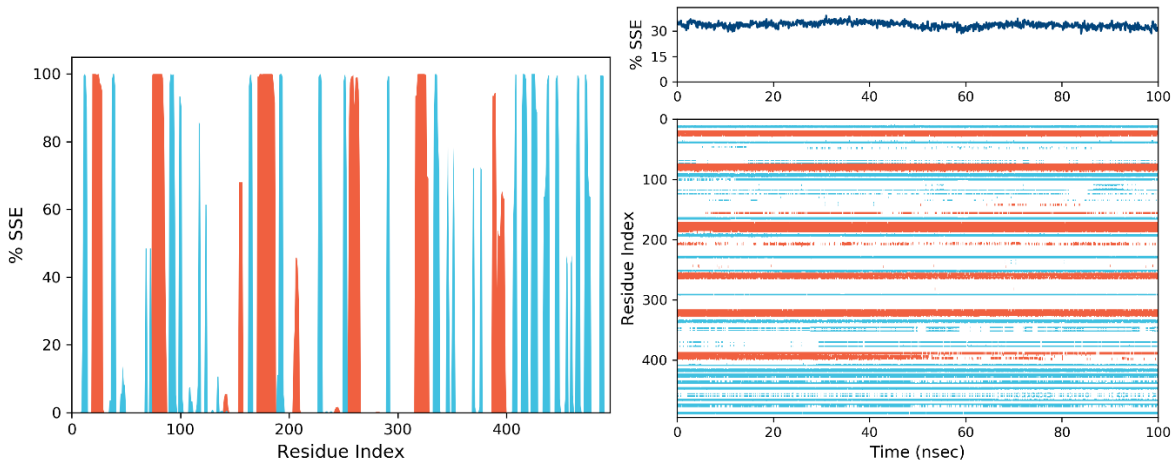

Figure 10. Protein Secondary structure Elements

Protein-Ligand Interactions

Interaction Analysis: The Interaction analysis identified key hydrogen bonds, hydrophobic contacts, ionic interactions, and water bridges between the protein and ligand. These interactions were stable and persistent throughout the simulation and contributed to the binding affinity and specificity of the ligand.

Hydrogen Bonds: Frequent hydrogen bonds were observed between the protein and ligand, with interactions involving both backbone and side-chain atoms. These hydrogen bonds are critical in stabilizing ligands within the binding pocket.

Hydrophobic Contacts: Persistent hydrophobic interactions were noted between the ligand and hydrophobic residues of the protein, further stabilizing the binding.

Ionic Interactions and Water Bridges: These interactions provide additional stabilization, enhancing the overall binding strength of the ligand to the protein (Figure 11).

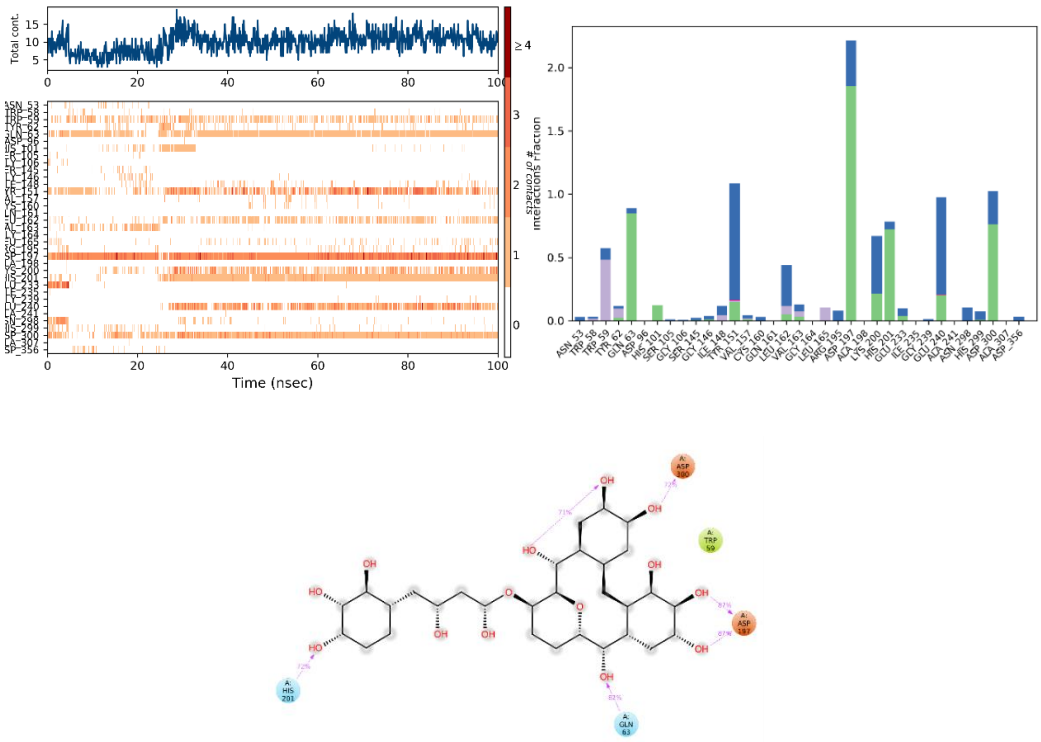

Figure 11. Protein-Ligand Interactions

Ligand Conformational Dynamics

Ligand Torsion Profile: The torsion profile of the rotatable bonds of the ligand indicates that the ligand maintained a relatively stable conformation within the binding pocket. Minor variations in torsion angles suggested that the ligand could slightly adapt its conformation to optimize the binding interactions (Figure 12).

Ligand Properties

Ligand Behavior: The calculated properties of the ligand, including RMSD, the radius of gyration (rGyr), intramolecular hydrogen bonds (intraHB), molecular surface area (MolSA), solvent accessible surface area (SASA), and polar surface area (PSA), provided a comprehensive understanding of the ligand's behavior and interaction dynamics. These properties remained consistent throughout the simulation, supporting the stability and efficacy of the ligand-binding

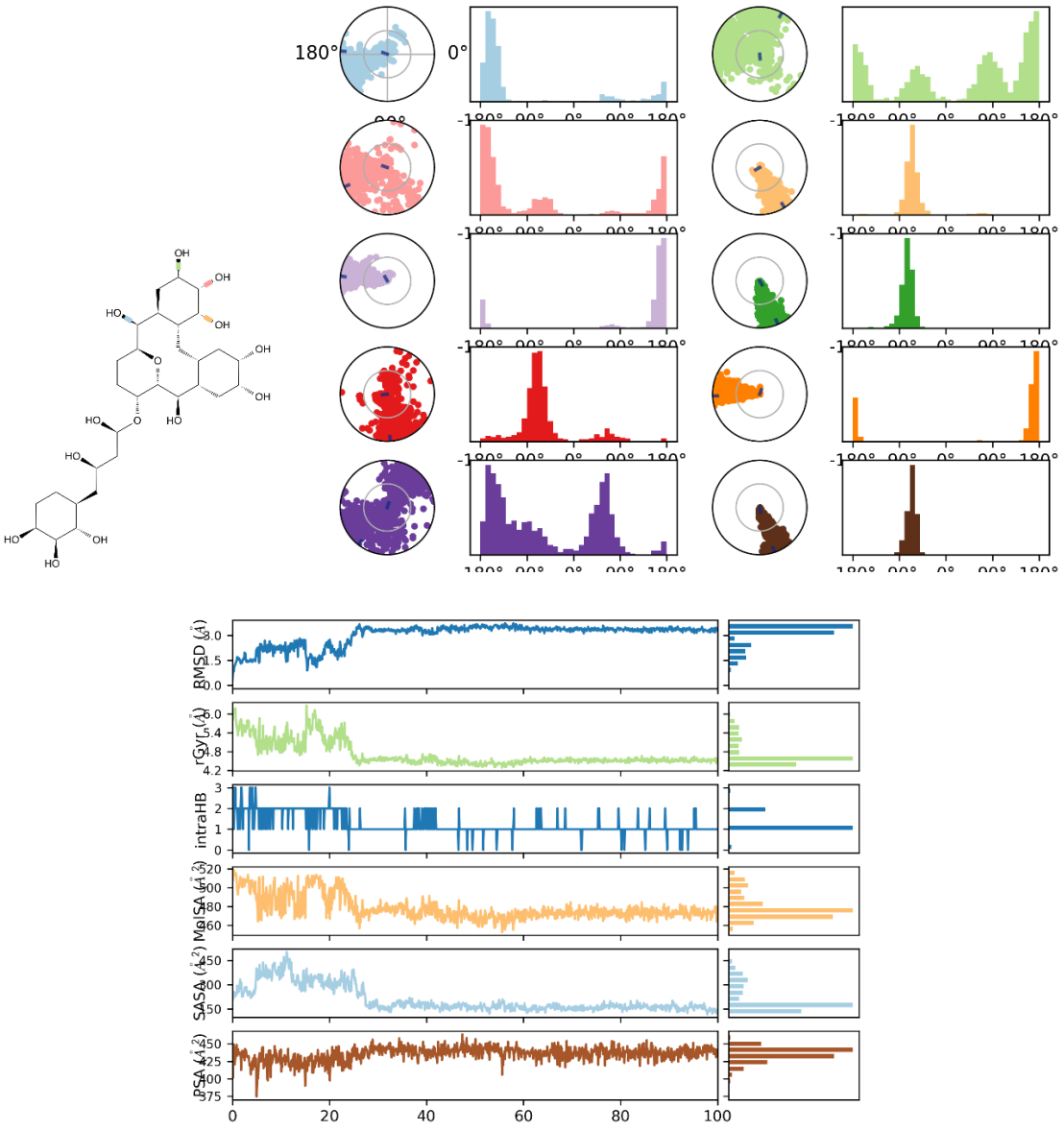

Figure 12. Ligand Conformational Dynamics

CONCLUSIONS

One flavonoid was isolated from the ethanolic extract of *S. zeylanicum* by column chromatography and its structure was confirmed by spectroscopic analysis. Molecular docking studies further suggested that SZ-I exhibits a multi-target therapeutic profile by forming stable interactions with several proteins in diabetes management. Molecular dynamics simulation validated the stability of SZ-I within the protein binding sites, demonstrating consistent structural integrity and dynamic interactions. Hydrogen bonds, hydrophobic contacts, and ionic interactions play critical roles in

stabilizing ligand-protein complexes, contributing to the overall efficacy of flavonoids as potential therapeutic agents for diabetes. The ligand maintained a stable conformation and exhibited consistent binding properties, indicating its potential as a multifunctional diabetes management candidate. The future scope of this research involves further in vivo validation of the isolated flavonoid SZ-I as a multitarget therapeutic agent for diabetes management, with potential exploration of its efficacy in clinical settings.

ACKNOWLEDGEMENTS

REFERENCES

Alam, S., Sarker, M. M. R., Sultana, T. N., Chowdhury, M. N. R., Rashid, M. A., Chaity, N. I., Zhao, C., Xiao, J., Hafez, E. E., Khan, S. A., & Mohamed, I. N. (2022). Antidiabetic Phytochemicals From Medicinal Plants: Prospective Candidates for New Drug Discovery and Development. *Front. Endocrinol.*, 13, 800714.

Aloke, C., Egwu, C. O., Aja, P. M., Obasi, N. A., Chukwu, J., Akumadu, B. O., Ogbu, P. N., & Achilonu, I. (2022). Current Advances in the Management of Diabetes Mellitus. *Biomedicines*, 10(10), 2436.

American Diabetes Association (2009). Diagnosis and classification of diabetes mellitus. *Diabetes Care*, 32(Suppl 1), S62–S67

Dokuparthi, S. K., & Reddy, T. R. M. (2021). Antioxidant and Nephroprotective Activity of Flavonoid Rich Fraction of *Alphonsea sclerocarpa* Thw. *Int. J. Pharm. Sci. Drug Res.*, 13(4), 384–394.

Dokuparthi, S. K., Banerjee, N., Kumar, A., Singamaneni, V., Giri, A. K., & Mukhopadhyay, S. (2014). Phytochemical investigation and evaluation of antimutagenic activity of the extract of *Cuscuta reflexa* Roxb. by Ames test. *Int. J. Pharm. Sci. Res.*, 5(8), 3430–3434.

Evans, M., Hicks, D., Patel, D., Patel, V., McEwan, P., & Dashora, U. (2020). Optimising the Benefits of SGLT2 Inhibitors for Type 1 Diabetes. *Diabetes Therapy*, 11(1), 37–52.

Faseela, V. A., & Maheshwari, P. (2024). Antioxidant and anticancer activity in leaf extracts of *Elaeocarpus serratus* (L.). *Ann. Phytomed.*, 13(1), 1–8.

Fatima, M., & Edupuganti, S. (2023). Comparative docking analysis of the phytochemicals isolated from *Landoltia punctata* (G. Mey.) Les & D.J. Crawford. *Eur. Chem. Bull.*, 12(10), 5420–5434.

Fatriansyah, J. F., Boanerges, A. G., Kurnianto, S. R., Pradana, A. F., Fadilah, & Surip, S. N. (2022). Molecular Dynamics Simulation of Ligands from *Anredera cordifolia* (Binahong) to the Main Protease (Mpro) of SARS-CoV-2. *J. Trop. Med.*, 2022, 1178228.

Galicia-Garcia, U., Benito-Vicente, A., Jebari, S., Larrea-Sebal, A., Siddiqi, H., Uribe, K. B., Ostolaza, H., & Martín, C. (2020). Pathophysiology of Type 2 Diabetes Mellitus. *Int. J. of Molecular Sciences*, 21(17), 6275.

Govindarajan, M., & Benelli, G. (2016). α-Humulene and β-elemene from *Syzygium zeylanicum* (Myrtaceae) essential oil: Highly effective and eco-friendly larvicides against *Anopheles subpictus*, *Aedes albopictus*, and *Culex tritaeniorhynchus* (Diptera: Culicidae). *Parasitology Research*, 115(7), 2771-2778.

Khan, M. A. B., Hashim, M. J., King, J. K., Govender, R. D., Mustafa, H., & Al Kaabi, J. (2020). Epidemiology of Type 2 Diabetes - Global Burden of Disease and Forecasted Trends. *J. of Epidemiology and Global Health*, 10(1), 107–111.

Khawandanah, J. (2019). Double or hybrid diabetes: A systematic review on disease prevalence, characteristics and risk factors. *Nutr. Diabetes*, 9, 33.

Macalalad, M. A. B., & Gonzales, A. A., 3rd. (2023). In Silico Screening and Identification of Antidiabetic Inhibitors Sourced from Phytochemicals of Philippine Plants against Four Protein Targets of Diabetes (PTP1B, DPP-4, SGLT-2, and FBPase). *Molecules*, 28(14), 5301.

Madej, T., Lanczycki, C. J., Zhang, D., Thiessen, P. A., Geer, R. C., Marchler-Bauer, A., & Bryant, S. H. (2014). MMDB and VAST+: tracking structural similarities between macromolecular complexes. *Nucleic Acids Res.*, 42(Database issue).

Nair, G. A., & Maheshwari, P. (2024). In vitro antioxidant and antidiabetic activity in leaf extracts of *Syzygium zeylanicum* (L.) DC. *Ann. Phytomed.*, 13(1), 627–634.

Nguyen, M.-T., Bui, T.-B.-H., Pham, V.-H., Tran, M.-D., & Nguyen, Q.-V. (2024). *Syzygium zeylanicum* (L.) DC. polyphenols exhibit anti-diabetic activity by modulation of ACC1, SGLT1, and GLP-1 genes and restoration of gut microbiota in overfeeding and high glucose exposure-induced diabetic zebrafish. *J. of Functional Foods*, 112, 105921.

Nomi, Y., Shimizu, S., Sone, Y., Tuyet, M. T., Pham, G. T., Kamiyama, M., Shibamoto, T., Shindo, K., & Otsuka, Y. (2012). Isolation and antioxidant activity of Zeylaniin A, a new macrocyclic ellagitannin from *Syzygium zeylanicum* leaves. *J. of Agricultural and Food Chemistry*, 60(41), 10263-10269.

Ota, A., & Ulrih, N. P. (2017). An Overview of Herbal Products and Secondary Metabolites Used for Management of Type Two Diabetes. *Front. Pharmacol.*, 8, 436. https://doi.org/10.3389/fphar.2017.00436

Saeedi, P., Petersohn, I., Salpea, P., Malanda, B., Karuranga, S., Unwin, N., Colagiuri, S., Guariguata, L., Motala, A. A., Ogurtsova, K., Shaw, J. E., Bright, D., Williams, R., & IDF Diabetes Atlas Committee (2019). Global and regional diabetes prevalence estimates for 2019 and projections for 2030 and 2045: Results from the International Diabetes Federation Diabetes Atlas, 9th edition. *Diabetes Res. and Clinical Practice*, 157, 107843.

Salo-Ahen, O. M. H., Alanko, I., Bhadane, R., Bonvin, A. M. J. J., Honorato, R. V., Hossain, S., et al. (2021). Molecular Dynamics Simulations in Drug Discovery and Pharmaceutical Development. *Processes*, 9(1), 71

Sanagala, V. M., Porika, R., Edupuganti, S., Dokuparthi, S. K., & Biman, K. K. (2024). Molecular Docking Evaluation of Phytochemicals in Fruits of *Terminalia pallida* Brandis: Implication on Immunomodulation. *Trop. J. Nat. Prod. Res.*, 8(5), 7106–7113.

Shilpa, K. J., & Krishnakumar, G. (2023). Comparative study on the antidiabetic activity of the bark extracts of *Syzygium caryophyllatum* (L.) Alston and *Syzygium zeylanicum* (L.) DC. *J. of Phytopharmacology*, 12(5), 326-333.

Singamaneni, V., Dokuparthi, S. K., Banerjee, N., Kumar, A., & Chakrabarti, T. (2020). Phytochemical Investigation and Antimutagenic Potential of Ethanolic Extracts of *Emblica officinalis*, *Terminalia chebula*, and *Terminalia bellirica*. *NPJ*, 10(4), 488–494.

Thabet, H. K., Ragab, A., Imran, M., Helal, M. H., Alaqel, S. I., Alshehri, A., Ash Mohd, A. A., Alshammari, S. S., Ammar, Y. A., & Abusaif, M. S. (2024). Innovation of 6-sulfonamide-2H-chromene derivatives as antidiabetic agents targeting α-amylase, α-glycosidase, and PPAR-γ inhibitors with in silico molecular docking simulation. *RSC Adv.*, 14, 15691-15705.

Weinberg Sibony, R., Segev, O., Dor, S., & Raz, I. (2023). Drug Therapies for Diabetes. *Int. J. of Molecular Sciences*, 24(24), 17147.